Cement and Concrete Research 40 (2010) 1009–1022

Contents lists available at ScienceDirect

Cement and Concrete Research

journal homepage: http://ees.elsevier.com/CEMCON/default.asp

Impact of chloride on the mineralogy of hydrated Portland cement systems

Magdalena Balonis [a,*], Barbara Lothenbach [b], Gwenn Le Saout [b,c], Fredrik P. Glasser [a]

[a] Department of Chemistry, Meston Building, University of Aberdeen, Aberdeen, AB24 3UE Scotland, UK
[b] EMPA, Swiss Federal Laboratories for Materials Testing and Research, Laboratory for Concrete & Construction Chemistry, Überlandstrasse 129, CH-8600 Dübendorf, Switzerland
[c] EPFL, Laboratory of Construction Materials, Swiss Federal Institute of Technology, Ecublens, 1015, Lausanne, Switzerland

ARTICLE INFO

Article history:
Received 20 October 2009
Accepted 3 March 2010

Keywords:
AFm phase
Chloride (D)
Characterization (B)
Thermodynamic calculations (B)
Corrosion (C)

ABSTRACT

Chloride ion is in part bound into ordinary Portland cement paste and modifies its mineralogy. To understand this a literature review of its impacts has been made and new experimental data were obtained. Phase pure preparations of Friedel's salt, $Ca_4Al_2(Cl)_{1.95}(OH)_{12.05}\cdot 4H_2O$, and Kuzel's salt, $Ca_4Al_2(Cl)(SO_4)_{0.5}(OH)_{12}\cdot 6H_2O$, were synthesized and their solubilities were measured at 5, 25, 55 and 85 °C. After equilibration, solid phases were analysed by X-ray diffraction while the aqueous solutions were analysed by atomic absorption spectroscopy and ion chromatography. The solid solutions and interactions of Friedel's salt with other AFm phases were determined at 25 °C experimentally and by calculations. In hydrated cements, anion sites in AFm are potentially occupied by OH, SO_4 and CO_3 ions whereas Cl may be introduced under service conditions. Chloride readily displaces hydroxide, sulfate and carbonate in the AFm structures. A comprehensive picture of phase relations of AFm phases and their binding capacity for chloride is provided for pH ~ 12 and 25 °C. The role of chloride in AFt formation and its relevance to corrosion of embedded steel are discussed in terms of calculated aqueous $[Cl^-]/[OH^-]$ molar ratios.

1. Introduction

The solid phases in hydrated cement systems consist mainly of portlandite and a gel-like phase, a calcium silicate hydrate termed C–S–H. Alumina combines with water, calcium and sulfate to form mainly AFt and AFm phases. Commercial Portland cement pastes contain ~5–15% of (AFm + AFt). Under service conditions, chloride ions may diffuse into the cement paste from the environment. Formation of Friedel's salt, containing essential chloride, is potentially a mechanism for retarding this diffusion and reducing aqueous $[Cl^-]/[OH^-]$ ratios.

AFm is shorthand for a family of hydrated calcium aluminate hydrate phases (aluminate–ferrite-monosubstituent phases). Its crystalline layer structure is derived from that of portlandite, $Ca(OH)_2$, but with one third of the Ca^{2+} ions replaced by a trivalent ion, nominally Al^{3+} or Fe^{3+}. The resulting charge imbalance gives the layers a positive charge which is compensated by intercalated anions (e.g. SO_4^{2-}, OH^-, Cl^- etc.); the remaining interlayer space is filled with H_2O. Its general formula is $[Ca_2(Al,Fe)(OH)_6]\cdot X\cdot xH_2O$, where X represents a monovalent ion or 0.5 of a divalent interlayer anion and x represents the number of water molecules. Studies have shown a multiplicity of AFm hydrate states and limited solid solution formation between various X anions [1–5]. Pöllmann described phase relations and ternary solid solutions between SO_4^{2-}, CO_3^{2-} and OH^- [1] as well as between Cl^-, OH^- and CO_3^{2-} [6] anions. Except for reported replacement of sulfate by hydroxide, chloride by hydroxide and chloride by carbonate' these anions do not form extensive AFm solid solutions and, from the mineralogical point of view, behave as separate phases. Moreover, chloride and sulfate AFm phases form an anion-ordered compound, 'Kuzel's salt', ideally with the 2:1 molar ratio of $[Cl]/[SO_4]$ [5,7]. AFm containing Cl^-, OH^- and CO_3^{2-} has been defined by mineralogists as 'hydrocalumite' [8,9]. SO_4-AFm (monosulfoaluminate) is also known as 'kuzelite' [10,11] whereas Cl-AFm is termed 'Friedel's salt' [12,13].

In commercial cements, the constitution of AFm is historically defined as containing OH^- and SO_4^{2-} in anion positions. But under service conditions or when calcium carbonate is added, the AFm phase may also contain carbonate and form monocarboaluminate (CO_3-AFm) or at very low-carbonate contents' hemicarboaluminate (AFm containing OH^- and CO_3^{2-} with the 2:1 molar ratio of $[OH]/[CO_3]$) [2,14]. Carbonate can be also introduced from unavoidable pre-hydration and carbonation during grinding, transport, and storage.

Chloride may enter cementitious systems in various ways, through the mixing water or from the service environment [15–18]. When chloride diffuses into the system from an external source, the resulting diffusion profile has a shape similar as predicted from Fick's laws [19]. Although the diffusion process is affected by other factors including ion exchange and chloride binding into the C–S–H and the AFm phase(s); the AFm serves as an important "sink" for chloride ions. This process has been studied extensively in the past [4,20–39] but conditions are not always well related to the environment in hydrated cements. The underlying mechanisms of chloride binding in cement systems are complex as several different processes act simultaneously. For example, chloride ions may interact with hydrated

* Corresponding author.
E-mail address: m.balonis@abdn.ac.uk (M. Balonis).

0008-8846/$ – see front matter © 2010 Elsevier Ltd. All rights reserved.
doi:10.1016/j.cemconres.2010.03.002

cement forming chloroaluminate phases, such as Friedel's, Kuzel's salt and solid solutions with other AFm phases [4,5,12,40–42] but can also be chemisorbed by C–S–H [17,25,38,43,44].

Chloride in cement paste has been widely studied because of its impact on the corrosion of steel in reinforced concrete. Two important parameters determining the risk of chloride-induced corrosion are believed to be: (i) the ratio of concentrations of chloride and hydroxyl ions in the pore solution and (ii) the diffusivity of chloride ions through cover concrete [45,46]. Assessments of the corrosion threshold at which chloride ions depassivate steel are related to $[Cl^-]/[OH^-]$ ratios in the pore solution [46–48]. Only the unbound fraction of the chloride dissolved in the aqueous phase of the concrete is deemed to interact destructively with the passivating layer on steel. Thus it is worthwhile to have precise information, preferably from non-destructive techniques, on the partition of chloride between "free" and "bound" states.

Thermodynamics provides a powerful tool to characterise the phase constitution of cementitious systems [14,49–52]. Geochemical modelling software such as GEMS enables calculation of the stable phase assemblage as a function of reactant composition, temperature and pressure. However thermodynamic calculations require a database of thermodynamic properties of cement substances. A key purpose of this research has been to extend the database for cementitious substances [53] with respect to chloride and determine the binding power of AFm for Cl in competition with hydroxide, sulfate and carbonate. Thermodynamic properties of chloride hydrates: Friedel's salt and Kuzel's salt have been determined. Investigations of solid solutions and calculations of competition between chloride and carbonate were performed and compared with experimental data.

2. Methods

2.1. Synthesis of chloride–aluminate hydrates

2.1.1. Friedel's salt

Tricalcium aluminate, $3CaO \cdot Al_2O_3$, was made by heating together a 3:1 molar ratio of reagent grades of $CaCO_3$ and Al_2O_3 at 1400 °C. The heating was done in Pt crucibles and continued, with intermediate grinding of the product, until X-ray powder diffraction revealed that the product was phase pure. Portions of this solid were mixed with weighted amounts of reagent grade $CaCl_2 \cdot 2H_2O$ (molar ratio of $C_3A:CaCl_2 = 1:1$). The water content of $CaCl_2 \cdot 2H_2O$ was confirmed thermogravimetrically. The precursors were added to double distilled, CO_2-free water, at a w/s (water to solid) ratio ~10, and tightly sealed into plastic containers to prevent CO_2 uptake. Samples were equilibrated with agitation for at least 28 days at 23 ± 2 °C.

2.1.2. Kuzel's salt

C_3A, $CaCl_2 \cdot 2H_2O$ and $CaSO_4$ were mixed in stoichiometric amounts and slurried in double distilled, CO_2-free water at a water/solid ratio of ~10. The mixture was equilibrated with agitation for 3 months at 23 ± 2 °C. Thereafter the solid was filtered under nitrogen atmosphere and dried in a desiccator over saturated calcium chloride. The resulting bulk solid gave an X-ray powder pattern corresponding to Kuzel's salt, $Ca_4Al_2(SO_4)_{0.5}(Cl)\ (OH)_{12} \cdot 6H_2O$, with a basal spacing $d = 8.32$ Å.

2.1.3. Solid solutions amongst AFm phases

Samples were synthesized from initial supersaturation at 23 ± 2 °C. Stoichiometric amounts of appropriate reactants were mixed and slurried in double distilled, CO_2-free water to a w/s ratio of ~10. The mixture was equilibrated with agitation for 3 months, then dried over saturated calcium chloride (35% RH) and analysed by XRD.

2.1.4. Cl-ettringite

Attempts to prepare chloride AFt were not successful. Mixtures of the appropriate composition, starting from C_3A and $CaCl_2$ and reacted at 5° and 25 °C, instead formed Friedel's salt. Preparations made using the so-called sucrose method, to enhance Ca solubility, gave an X-ray amorphous product. Damidot et al. [54] made similar observations but claimed possible metastable existence of chloride ettringite at 25 °C. Pöllmann [55] attempted the synthesis at room temperature and reported that the chloride content of the product was <0.7% (compared with theoretical 17.7%). Chloride ettringite has been reported to occur stably below 0 °C [56–60], but the conditions of the title study did not extend to <5 °C.

2.2. Analysis of pH, cation and anion concentrations in solutions

The pH was determined by a METTLER TOLEDO ion selective electrode INLAB 413, which simultaneously measures aqueous pH and temperature. The pH-meter was calibrated at 25 °C using a 3-point calibration with certified commercial buffers at pH 9.21, 10.00 and 13.00. For the samples equilibrated at 5, 55 and 85 °C, pH was determined at room temperature and later corrected by the calculation to the measurement temperature (pH buffer solutions were provided with information about the temperature dependence of pH, enabling correction).

Aqueous sulfate and chloride concentrations were measured using DX-120 IC ion chromatograph equipped with a 4 mm ion exchange analytical column.

Aqueous calcium and aluminium were analysed by atomic adsorption spectroscopy using a Varian SpectrAA 10 flame AAS unit. A nitrous oxide/acetylene flame was used for aluminium and air/acetylene flame for calcium. In the determination of calcium a solution of $LaCl_3$ (of final concentration ~10,000 ppm) was employed as a release agent. For aluminium, KCl at a 2500 ppm K^+ was added to suppress ionisation. Calcium was measured at a wavelength 422.7 nm and aluminium at 309.3 nm. Standards prepared from 1000 mg/L 'Spectrosol' solutions (VWR chemicals) were used for calibration.

2.3. X-ray diffraction (XRD)

A Bruker D8 advance powder diffractometer was used for X-ray: characteristics of Friedel's salt and Kuzel's salt, measurement of Friedel's salt-hydroxy AFm solid solutions and analysis of experimental data on phase assemblages (carbonate-free and carbonate-containing systems) reported in Section 4. Data were collected using CuKα radiation (λ = 1.54 Å) at room temperature (23 ± 2 °C).

Friedel's salt–monosulfoaluminate and Friedel's salt–monocarboaluminate phase mixtures/solid solutions were measured at room temperature (23 ± 2 °C) on the PANalytical X'Pert Pro MPD diffractometer using CuKα radiation (λ = 1.54 Å) and an X'Celerator detector. Powder samples were loaded sideways to the sample holder to reduce preferred orientation effects in samples with platy crystals, e.g. portlandite or AFm. ICSD codes (Inorganic Crystal Structure Database, version 2009/1) were used for Rietveld refinement of Friedel's salt (for the rhombohedral phase: ICSD: 88617, 51890; for the monoclinic phase ICSD: 62363). When attempts to apply the structure file to refine were unsuccessful (as for the monoclinic phase of Friedel's salt ICSD 62363) a Le Bail simulation fit was used.

2.4. Solubility product determination and thermodynamic modelling

The solid products, Friedel's salt (ideally $Ca_4Al_2Cl_2(OH)_{12} \cdot 4H_2O$), and Kuzel's salt ($Ca_4Al_2(SO_4)_{0.5}(Cl)(OH)_{12} \cdot 6H_2O$) were dried and dispersed in double distilled water and equilibrated at 5, 25, 55 and 85 °C. After equilibration at a w/s ratio ~30, ion concentrations were measured using AAS and ion chromatography. Aqueous ion activities and speciation were calculated using the GEMS database, by applying the extended Debye–Hückel equation to correct for activities [53]. Measured concentrations of Ca, Al, Cl and sulfate were used as input to calculate the solubility products.

All calculations were carried out using the GEMS-PSI [61] software package. GEMS is a broad-purpose geochemical modelling code which uses Gibbs energy minimization criterion and computes equilibrium phase assemblage and speciation in a complex chemical system from its total bulk elemental composition. Chemical interactions involving solids, solid solutions, and aqueous electrolyte are considered simultaneously. Input data for cement hydrates were taken from Matschei et al. [53] and the title study.

The properties of chloride-containing hydrates (Sections 3.1, 3.2) used in the calculations are presented in Table 1. Experimental solubility products were determined using samples equilibrated for 12 months (Tables 2, 3; values indicated in italic).

The solubility of Friedel's and Kuzel's salt was measured between 5 and 85 °C and thus data to describe the solubility as a function of temperature could be derived. From the solubility products calculated at the different temperatures, the thermodynamic properties were calculated using the built-in 3-term temperature extrapolation, to obtain the temperature dependent logK_T function (Eqs. (1)–(4))

$$\log K_T = A_0 + \frac{A_2}{T} + A_3 \ln T \tag{1}$$

$$A_0 = \frac{0.4343}{R} \cdot \left[\Delta_r S^\circ_{T_0} - \Delta_r Cp^\circ_{T_0}(1 + \ln T_0)\right] \tag{2}$$

$$A_2 = \frac{0.4343}{R} \cdot \left(\Delta_r H^0_{T_0} - \Delta_r Cp^\circ_{T_0} T_0\right) \tag{3}$$

$$A_3 = \frac{0.4343}{R} \cdot \Delta_r Cp^\circ_{T_0}. \tag{4}$$

The entropy S° was adjusted to obtain the best fit between the measured solubility data at different temperatures and the calculated solubility products. As only a few solubility measurements were available, only the entropy was fitted, while the heat capacities C°_p were estimated based on the reference reactions with the structurally similar monosulfoaluminate with known C°_p [53]. If such reference reactions involve only solids and no "free" water, the change in heat capacity and the entropy is approximately zero. As shown in the literature [53,63] this approximation has been successfully applied in the past.

3. Results

3.1. Friedel's salt

The preparation gave an X-ray powder pattern at 25 ± 2 °C corresponding to that reported for Friedel's salt with basal spacing d = 7.93 Å. In some preparations, Friedel's salt giving a basal spacing of 7.89 Å and 7.83 Å was found. The lowered spacing is probably due to presence of the rhombohedral (R) phase. At room temperature Friedel's salt is monoclinic (M) with a basal spacing around 7.91 Å [42] but above ~35 °C [7,13,64] it is reported to transform to rhombohedral symmetry (basal spacing 7.77 Å [42]). It is probable that, depending upon bulk composition and the OH/Cl ratio of the solid the transformation temperature will vary.

Rietveld analysis of Friedel's salt prepared by mixing C_3A:$CaCl_2$ = 1:1 revealed that even at room temperature, preparations consisted of a mixture of phases, approximately 93% monoclinic and 7% rhombohedral. The existence of two phases over a range of temperatures can be explained by differing extents of substitution of Cl by OH, thereby creating a stable range of coexistence for solid solutions based on R and M phases.

Independent bulk chemical analysis of the chloride content disclosed that the formula of the solid, made according to the method given, was $Ca_4Al_2Cl_{1.95}(OH)_{12.05}\cdot 4H_2O$. Previous researchers [42,65] reported that, by reacting C_3A and $CaCl_2$ in 1:1 stoichiometric amounts with water, the maximum chloride content obtained for the final product was ~95% of the theoretical chloride content. In the title study, about 2.5% OH was substituted for Cl in preparations made at pH ~ 12. Solubility data are presented in Table 2.

Solubility products (K_{so}) of Friedel's salt were calculated according to the dissolution reactions presented in Eq. (5).

$$Ca_4Al_2(OH)_{12.05}(Cl)_{1.95}\cdot 4H_2O = 4Ca^{2+} + 2AlO_2^- + 1.95Cl^- + 4.05OH^- + 8H_2O \tag{5}$$

Other numerical values of the solubility products of 'Friedel's salt' have been reported in the literature. Birnin-Yauri [12,65] given values of logK_{so} between −24.79 and −27.10. Hobbs [42] estimated logK_{so} as −27.57 ± 0.86 and Bothe [66] calculated the solubility product to be within the range −28.8 < logK_{so} < −27.6.

3.2. Kuzel's salt

Kuzel's salt $Ca_4Al_2(SO_4)_{0.5}(Cl)(OH)_{12}\cdot 6H_2O$ gave an X-ray powder pattern at 25 ± 2 °C with a basal spacing of d = 8.32 Å. It dissolves incongruently; solubility data are presented in Table 3. After dissolution, the X-ray diffraction pattern of the solid disclosed the presence of Kuzel's salt together with monosulfoaluminate and Friedel's salt. The stability of Kuzel's salt relative to mixtures of monosulfoaluminate and Friedel's salt is considered to be proven because the two AFm end members, mixed in the 1:1 ratio, react at 25 ± 2 °C to yield Kuzel's salt. That is, at 25 °C, two different phase assemblages react and converge on the same final state: Kuzel's salt [5].

Solubility products (K_{so}) of Kuzel's salt were calculated according to the dissolution reaction presented in Eq. (6).

$$Ca_4Al_2(SO_4)_{0.5}(Cl)(OH)_{12}\cdot 6H_2O = 4Ca^{2+} + 2AlO_2^- + Cl^- + 0.5SO_4^{2-} + 4OH^- + 10H_2O \tag{6}$$

Data for the solubility product of Kuzel's salt have not been published previously in the literature. However from the solubility data given by Glasser et al. [5] we estimated logK_{so} to be −28.54.

3.3. AFm solid solutions

Solid solutions are frequently encountered in cementitious systems [2,51,67–70] and result from the partial substitution of one or more types of atoms or ions in a single homogeneous crystalline structure [71]. If the size, shape and charge of the host and substituent ions are similar, solid solution may be ideal but the larger the differences, the stronger is the tendency to non-ideality [71,72] and the tendency to form miscibility

Table 1
Standard molar thermodynamic properties of Friedel's salt and Kuzel's salt at 25 °C.

	logK_{s0}	$\Delta_f G^\circ$ [kJ/mol]	$\Delta_f H^\circ$ [kJ/mol]	S° [J/K/mol]	a_0 [J/(mol K)]	a_1 [J/(mol K^2)]	a_2 [J K/mol]	a_3 [J/(mol K$^{0.5}$)]	C°_p [J/K mol]	d[a] [kg/m^3]
$C_4ACl_{1.95}H_{10.025}$	−27.69	−6814.6	−7625	731	498	0.89	−2.03e+06	1503	829	2064
$C_4As_{0.5}ClH_{12}$	−28.53	−7533.3	−8587	820	557	1.14	−1.01e+06	751.5	929	2114

K_{S0}-thermodynamic equilibrium constant at T_o = 298 K; $\Delta_f G^\circ$ − standard molar Gibbs energy of formation at T_o = 298 K; $\Delta_f H^\circ$ − standard molar enthalpy at T_o = 298 K; S° − standard molar absolute entropy at T_o = 298 K; a_0, a_1, a_2, a_3 temperature independent empirical parameters characteristic of each solid; C°_p − heat capacity at T_o = 298 K.
[a] Density values taken from [62].

Table 2
Solubility data for Friedel's salt — $Ca_4Al_2(OH)_{12.05}(Cl)_{1.95}\cdot 4H_2O$.

Temp. [°C]	Ca [mmol/l]	Al [mmol/l]	Cl [mmol/l]	logK_{so}	pH measured	Equilibrium pH calc. by GEMS	Age-months	Phases present after dissolution
5	7.33	3.96	3.77	−29.53	12.40[a]	12.51	1	n.d.
5	7.30	2.93	3.86	−29.24	12.45[a]	12.56	3	Fs_{ss}
5	7.29	2.90	3.76	−29.24	12.45[a]	12.57	6	n.d.
5	7.20	2.85	3.70	−29.28	12.43[a]	12.56	8	Fs_{ss}
5	7.25	2.89	3.72	−29.26	12.44[a]	12.57	12	Fs_{ss}
25	9.19	4.52	4.95	−27.87	12.00	11.90	1	n.d.
25	9.09	2.48	4.89	−27.63	12.01	11.98	1	Fs_{ss}
25	9.13	2.63	4.97	−27.59	12.01	11.97	3	Fs_{ss}
25	8.92	2.73	4.89	−27.66	11.99	11.96	3	n.d.
25	8.95	2.35	4.98	−27.72	12.00	11.97	6	Fs_{ss}
25	9.11	2.78	5.02	−27.57	11.96	11.96	6	Fs_{ss}
25	8.99	2.69	4.98	−27.64	11.98	11.96	8	n.d.
25	8.77	2.97	5.50	−27.71	11.94	11.90	8	Fs_{ss}
25	*8.88*	*2.70*	*5.70*	*−27.69*	*11.94*	*11.92*	*12*	*Fs_{ss}*
25	8.82	2.39	5.79	−27.78	11.93	11.92	12	n.d.
55	13.25	2.31	14.31	−26.94	11.08[a]	10.99	3	Fs_{ss}, HG
55	13.66	2.45	15.10	−26.83	11.08[a]	10.98	6	n.d.
55	13.73	2.28	15.25	−26.85	11.09[a]	10.99	8	Fs_{ss}, HG
55	13.73	2.70	15.43	−26.82	11.06[a]	10.97	12	n.d.
85	16.05	2.90	19.46	−26.96	10.22[a]	10.24	3	Fs_{ss}, HG
85	16.68	2.57	19.06	−26.77	10.21[a]	10.32	6	n.d.
85	16.58	2.50	19.20	−26.83	10.20[a]	10.31	8	Fs_{ss}, HG
85	16.60	2.54	19.69	−26.86	10.19[a]	10.29	12	n.d.

Abbreviations: Fs_{ss}— Friedel's salt in solid solution with OH-AFm, HG—hydrogarnet, n.d.—not determined. Italicised value from 12 month equilibration was used as an input in Table 1.
[a] pH measured at 25 °C and corrected by calculation to measurement temperature (see Section 2.2).

gaps. Solid solution can provide thermodynamic stabilisation for particular compositions or range of compositions and may reflect in a non-ideal trend of dissolved ion concentrations. Solid solutions are often more stable than mechanical mixtures of the end members and thus stabilise the formation of the solid solution with respect to other solid phase assemblages.

3.3.1. Friedel's salt and hydroxy AFm phase

To investigate whether solid solutions are formed, a series of solids were either analysed by XRD (Fig. 1) wet, or following drying over saturated calcium chloride (35% RH) (Fig. 2).

Solid solution formation between Friedel's salt (basal spacing $d = 7.93$ Å) and hydroxy AFm (basal spacing $d = 7.99$ Å) was investigated in the range 0–1 Cl/(Cl + OH). The extent of the miscibility gap has been variously reported by Hobbs [42], to be below ratio 0.33 Cl/(Cl + OH), by Pöllmann and Kuzel [73] to be below 0.34 Cl/(Cl + OH), by Birnin-Yauri [65], below ratio 0.3 Cl/(Cl + OH) and by Roberts [74], below ratio 0.4 Cl/(Cl + OH). However, and in contrast, Turriziani [75] claimed formation of complete solid solution. Previous researchers based the evidence of incomplete solid solution on the observation that changing bulk composition caused two separate X-ray reflections' one for Friedel's salt another one for the high water variant of hydroxy AFm with a basal spacing $d \sim 10.7$ Å. In this investigation, only the lower

Table 3
Solubility data for Kuzel's salt — $Ca_4Al_2(SO_4)_{0.5}(Cl)(OH)_{12}\cdot 6H_2O$.

Temp. [°C]	Ca [mmol/l]	Al [mmol/l]	Cl [mmol/l]	SO_4 [mmol/l]	logK_{so}	pH measured	Equilibrium pH calc. by GEMS	Age- months	Phases present after dissolution
5	5.25	3.26	3.85	0.005[a]	−30.45	12.34[b]	12.20	1	Ks, Fs, Ms
5	5.47	3.16	3.89	0.005[a]	−30.19	12.33[b]	12.26	3	Ks, Fs, Ms
5	5.45	3.10	3.99	0.005[a]	−30.23	12.35[b]	12.25	6	n.d.
5	5.35	3.16	4.10	0.005[a]	−30.40	12.31[b]	12.21	8	Ks, Ms, Fs
5	5.35	3.19	3.96	0.005[a]	−30.35	12.26	12.22	12	n.d.
25	7.65	4.14	4.01	0.009[a]	−28.53	11.76	11.77	1	Ks, Ms, Fs
25	8.73	2.61	5.96	0.009[a]	−28.25	11.77	11.86	3	Ks, Ms, Fs
25	8.88	2.21	6.22	0.009[a]	−28.28	11.80	11.88	3	Ks, Ms, Fs
25	8.64	2.26	5.89	0.009[a]	−28.35	11.76	11.87	6	Ks, Ms, Fs
25	8.66	2.39	5.90	0.009[a]	−28.32	11.88	11.87	6	n.d.
25	8.66	2.43	5.93	0.009[a]	−28.31	11.87	11.86	8	Ks, Ms, Fs
25	8.68	2.40	5.98	0.009[a]	−28.32	11.82	11.87	8	n.d.
25	*8.41*	*2.31*	*5.70*	*0.009*[a]	*−28.53*	*11.76*	*11.79*	*12*	*Ks, Ms, Fs*
25	8.21	2.51	5.39	0.009[a]	−28.51	11.74	11.86	12	n.d.
55	13.46	3.30	11.99	0.25[a]	−26.64	11.07[b]	11.04	3	Ks, HG, Ms, Fs
55	12.71	3.31	11.38	0.25[a]	−26.84	11.05[b]	11.01	6	n.d.
55	13.15	3.20	12.02	0.25[a]	−26.77	11.08[b]	11.02	8	Ks, HG, Ms, Fs
55	12.88	3.49	11.89	0.25[a]	−26.82	11.02[b]	10.99	12	n.d.
85	17.03	3.54	16.94	1.31[a]	−26.50	10.41[b]	10.32	3	Ks, HG, Ms, Fs
85	17.49	3.71	16.51	1.31[a]	−26.39	10.36[b]	10.34	6	Ks, HG, Ms, Fs
85	18.20	3.48	17.55	1.31[a]	−26.32	10.37[b]	10.35	8	Ks, HG, Ms, Fs
85	18.15	3.55	17.41	1.31[a]	−26.31	10.37[b]	10.35	12	n.d.

Ks—Kuzel's salt, HG—hydrogarnet, Ms—monosulfoaluminate, Fs—Friedel's salt, n.d.—not determined. Italicised value from 12 month equilibration was used as an input in Table 1.
[a] Sulfate concentration determined assuming saturation with respect to monosulfoaluminate-data taken from Matschei et al. [53].
[b] pH measured at 25 °C and corrected by calculation to measurement temperature (see Section 2.2).

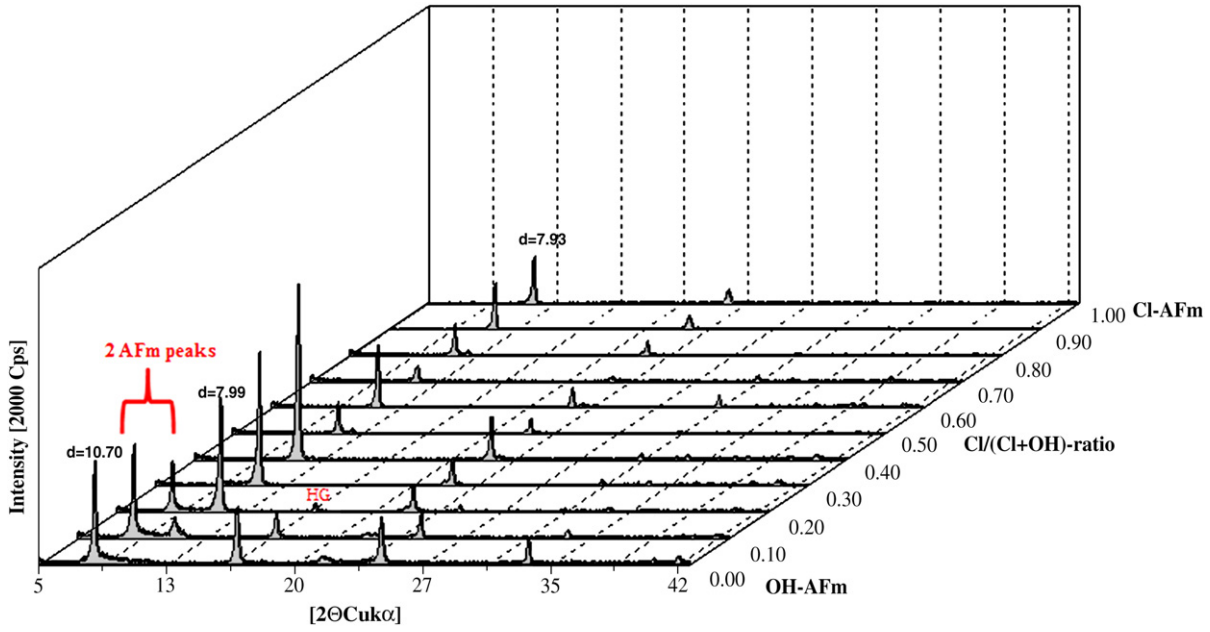

Fig. 1. Partial XRD patterns of the solid solution formation at 25 °C between Friedel's salt and hydroxy AFm: wet samples. Reflections marked as HG are attributed to hydrogarnet.

water phase, C_4AH_{13} ($Ca_4Al_2(OH)_{14}\cdot 6H_2O$), basal spacing $d=7.99$ Å, was found after drying at 35% RH (Fig. 2). Main reflections of chloride and hydroxy end members coincided (close to 2 theta 11.40°, Cu radiation) therefore to distinguish them peaks at ~2 theta 22° were analysed. For members of solid solution peaks at ~2 theta 22° were investigated by Rietveld refinement but the signal to noise ratio was too low to establish solid solution limits. To define the miscibility gap without artefacts introduced by drying, X-ray characterisation used wet samples covered with 'Mylar' foil to prevent water evaporation and prevent atmospheric carbonation. This preserved the higher water state of AFm; two separate peaks were observed in the region below ratio 0.2 Cl/(Cl + OH) (Fig. 1) Thus the coexisting solid solution of the (OH, Cl) AFm phases which are in different water states is inevitably incomplete. It is concluded that the presence of chloride stabilises the "$13H_2O$" state at the expense of the "$19H_2O$" state. A continuous solid solution between C_4AH_{13} and Cl-AFm (Friedel's salt) is not, however, precluded.

Dry (Cl, OH) AFm solid solution members were redispersed in double distilled water and equilibrated at 25 °C for 180 days. All the samples were periodically agitated. Aqueous solution compositions, measured after equilibration commencing from undersaturation, are presented in Table 4. Calcium, aluminium and chloride concentrations are plotted in Fig. 3(a, b).

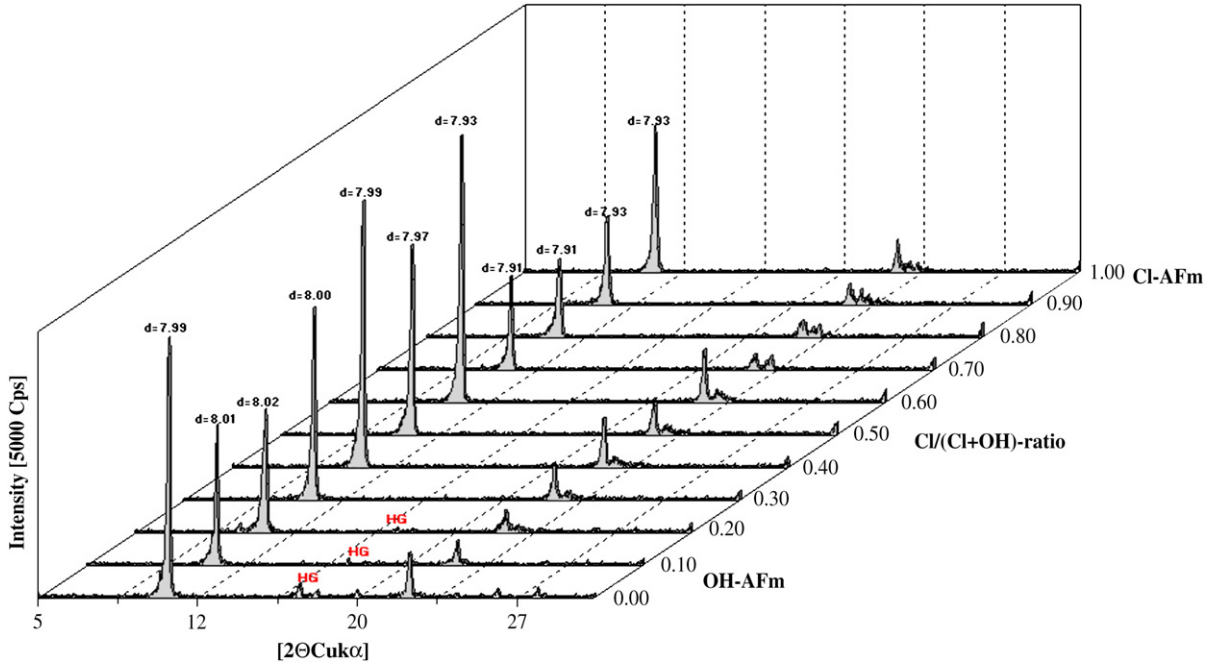

Fig. 2. Partial XRD patterns of the solid solution formation at 25 ± 2 °C between Friedel's salt and hydroxy AFm: samples dried at RH 35%. Reflections marked as HG are attributed to hydrogarnet.

Table 4
Aqueous solution compositions measured from undersaturation for samples between the hydroxy AFm (Cl/Al = 0) and the Friedel's salt (Cl/Al = 1) and with an excess of $CaCl_2$ (values > 1); at 25 ± 2 °C and after 180 days of equilibration. Data for hydrogarnet, $Ca_3Al_2(OH)_{12}$ are given for reference.

Calculated Cl/Al-ratio (total system)	Ca [mmol/l] (aq)	Al [mmol/l] (aq)	Cl [mmol/l] (aq)	pH	Solid phase at end of experiment
0.00	17.63	0.21	0.00	12.49	OH-AFm, HG, CH
0.10	17.19	0.24	0.72	12.47	FS_{ss}, HG
0.20	15.21	0.29	0.86	12.46	FS_{ss}, HG
0.30	12.68	0.79	1.29	12.41	Fs_{ss}, HG
0.40	10.53	1.87	1.73	12.33	FS_{ss}, HG(traces)
0.50	8.69	3.27	2.09	12.21	FS_{ss}
0.60	8.84	3.61	3.61	12.14	FS_{ss}
0.70	8.62	4.46	3.78	12.07	FS_{ss}
0.80	8.59	3.77	4.31	12.09	FS_{ss}
0.90	8.91	2.49	4.92	12.12	FS_{ss}
0.95	8.82	2.39	5.79	11.93	FS_{ss}
1.05	11.63	1.35	11.57	11.78	FS_{ss}
1.10	13.13	0.89	15.7	11.70	n.d.
1.20	16.78	0.93	24.5	11.62	n.d.
For pure hydrogarnet	6.31	5.07	0	11.81	HG

Abbreviations: FS_{ss} = solid solution between Cl-AFm and OH-AFm, CH = portlandite, HG = hydrogarnet (katoite); n.d. = not determined.

3.3.2. Friedel's salt and monosulfoaluminate phase

No solid solution was found between monosulfoaluminate and Friedel's salt: instead an ordered compound containing both mono and divalent anions, $Ca_4Al_2(SO_4)_{0.5}(Cl)(OH)_{12}\cdot 6H_2O$ (Kuzel's salt), was encountered (Fig. 4). These findings are similar to those reported by Stronach [76] who additionally found a slight solid solution between monosulfoaluminate and Friedel's salt. Solubility data for Kuzel's salt are presented in Section 3.2.

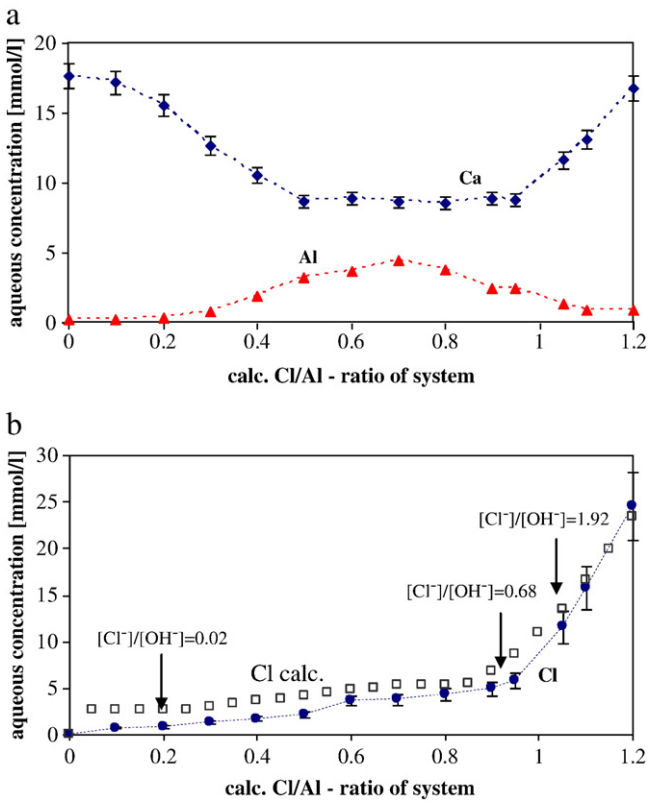

Fig. 3. (a). Equilibrium calcium and aluminium aqueous concentrations commencing from undersaturation for samples between hydroxy AFm (Cl/Al = 0) — Friedel's salt (Cl/Al = 1) and with an excess of calcium chloride (values > 1); at 25 ± 2 °C and after 180 days of equilibration. Error bars are shown for Ca. (b). Equilibrium chloride aqueous concentrations commencing from undersaturation for samples between hydroxy AFm, (Cl/Al = 0) and Friedel's salt (Cl/Al = 1) and with an excess of calcium chloride (values > 1); at 25 ± 2 °C and after 180 days of equilibration. Error bars are shown for Cl. Variations in the measured aqueous $[Cl^-]/[OH^-]$ ratios are shown at selected points: see Discussion. Open squares represent chloride concentrations calculated by GEMS.

3.3.3. Friedel's salt and monocarboaluminate phase

Extensive solid solution was found between Friedel's salt and monocarboaluminate (Fig. 5). A miscibility gap exists ≤0.1 Cl/(Cl + 1/2CO_3). One phase, Friedel's salt type, has a basal spacing $d = 7.72$ Å and the other, monocarboaluminate type, has $d = 7.50$ Å. This is in agreement with observations reported in the literature; Pöllmann [41] identified a miscibility gap ≤0.10 Cl and Hobbs [42] found a miscibility gap at ≤0.09 Cl. Calcite was found as an additional phase. Samples were redispersed in double distilled water and equilibrated at 25 °C for 180 days. All the preparations were periodically agitated. Analysis of the solubility data for particular members of solid solution as well as for some samples containing excess of calcium chloride is presented in Table 5. Aqueous: calcium, aluminium and chloride concentrations are plotted in Fig. 6(a, b).

4. AFm phase interactions

Thermodynamic modelling was performed on the AFm phases in the systems C_3A–$CaSO_4$–$CaCl_2$–H_2O and C_3A–$CaSO_4$–$CaCO_3$–$CaCl_2$–H_2O. A key purpose of the calculation was to determine the binding power of AFm for chloride *in competition with realistic concentrations of sulfate and carbonate* and compare calculated data on anion fractionation with experiment.

For modelling purposes, an ideal solid solution between Friedel's salt, hydroxy AFm and monocarboaluminate was assumed and agreed well with changes observed in the aqueous phases (Figs. 3(b), 6(b), 8(b), 10(b)). The calculations assume alkali-free conditions.

4.1. Carbonate-free system

The model results shown in Fig. 7, depict the sequence of phase changes occurring in AFm with increasing molar ratio of chloride to alumina. This depiction usefully simulates phase changes occurring when' for example' chloride ingresses hardened cement paste. Chloride, introduced in the calculation as $CaCl_2$, readily displaces sulfate from "monosulfoaluminate" (Fig. 7) which is in solid solution with hydroxy AFm, (designated as SO_4-AFm_{ss}) forming an intermediate compound Kuzel's salt, $Ca_4Al_2(SO_4)_{0.5}(Cl)(OH)_{12}\cdot 6H_2O$, at low $CaCl_2$ concentration (below molar ratio of $2Cl/Al_2O_3 \sim 0.70$) but Friedel's salt in solid solution with hydroxy AFm (designated as Friedel's $salt_{ss}$) at higher chloride concentration, above molar ratio $2Cl/Al_2O_3 \sim 0.70$.

The calculations are in accordance with experimental data reported by Hirao [25,77], Zibara [36], Csizmadia [21] and Kopecskó [26]. Sulfate ions, released from monosulfoaluminate, form ettringite and this additional ettringite formation results in significant increase in the molar volume of the solids, as shown in Fig. 8(a).

Experimental results on a phase assemblage containing 0.01 mol C_3A–0.01 mol $CaSO_4$–0.015 mol $Ca(OH)_2$ and 60 ml H_2O are shown in Fig. 9, plot 1; the phases formed were identified as monosulfoaluminate (marked as Ms) in solid solution with hydroxy AFm, portlandite (P) and minor amounts of ettringite. In the course of reaction with $CaCl_2$, phase changes occur (plots 2–4): sulfate is displaced from monosulfoaluminate and, at lower chloride contents, Kuzel's salt forms (marked as Ks on plots 2 and 3). At still higher chloride content (plot 4) Friedel's salt (in solid solution with hydroxy AFm), was found. Sulfate ions liberated from AFm form ettringite (marked as E in plots 1–4). Thus experiment confirms the calculated reaction sequence. Aqueous compositions (simulated and measured) are compared in Fig. 8(b) with generally satisfactory agreement. Note

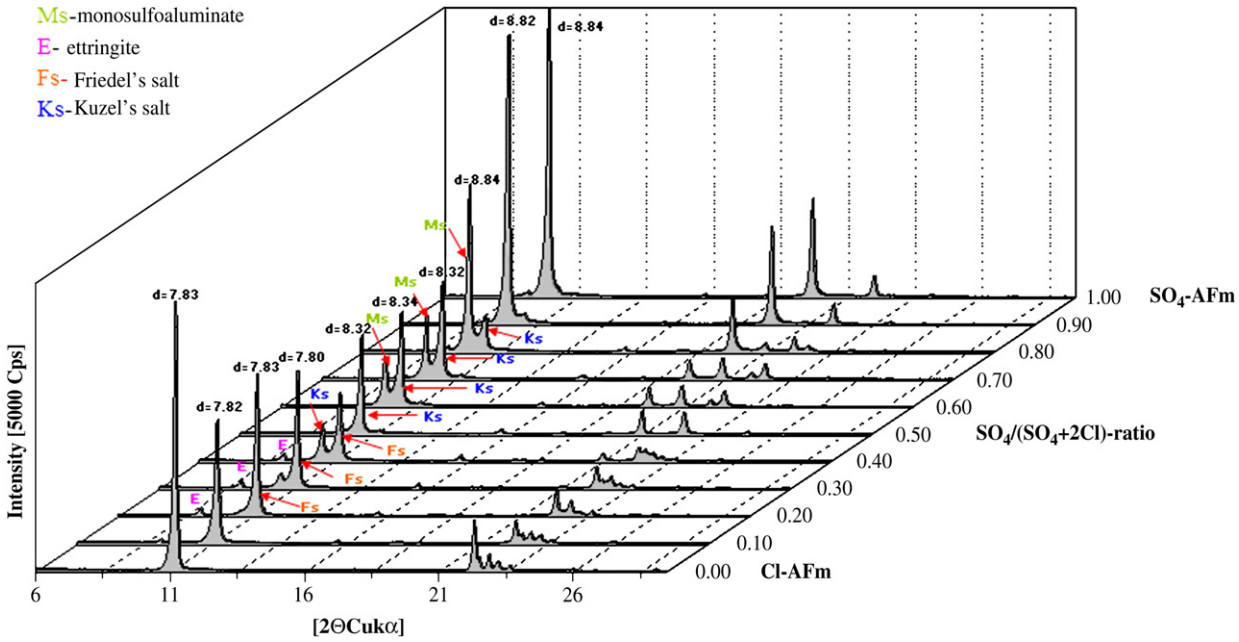

Fig. 4. Partial XRD patterns of mixtures between Friedel's salt and monosulfoaluminate at 25 ± 2 °C; note formation of Kuzel's salt at $SO_4/(SO_4 + 2Cl)$ ratio 0.5.

that the pH decreases in stepwise manner with rising $2Cl/Al_2O_3$ over the range of compositions included.

4.2. Carbonate-containing system

Calculated phase changes for the system C_3A–$CaSO_4$–$CaCl_2$–$CaCO_3$–H_2O are presented in Fig. 10(a). Calculations were done for mixtures of monocarboaluminate, portlandite and ettringite. With rising chloride content, carbonate ions in the AFm are substituted by chloride, forming Friedel's salt; the liberated carbonate ions are bound in calcite. Experimental verification was done by equilibrating for 45 days at 25 °C a mixture containing: 0.01 mol C_3A, 0.01 mol $CaSO_4$, 0.015 mol $Ca(OH)_2$, 0.0075 mol $CaCO_3$ and 60 ml H_2O. Fig. 11 shows the results. Initially-formed phases (plot 1) were identified as monocarboaluminate (marked as Mc) portlandite (P) and ettringite (E). In the course of admixing $CaCl_2$, a phase change occurs (plot 2). Friedel's salt appeared while carbonate, displaced from monocarboaluminate, forms calcite (marked as Cc). Thus calcite can be formed at constant carbonate content, without introduction of additional carbonate from an external source, by displacement from carbonate-containing AFm solids. Kuzel's salt does not appear because its formation is suppressed by the greater stability of monocarboaluminate. Volume changes in this case are much

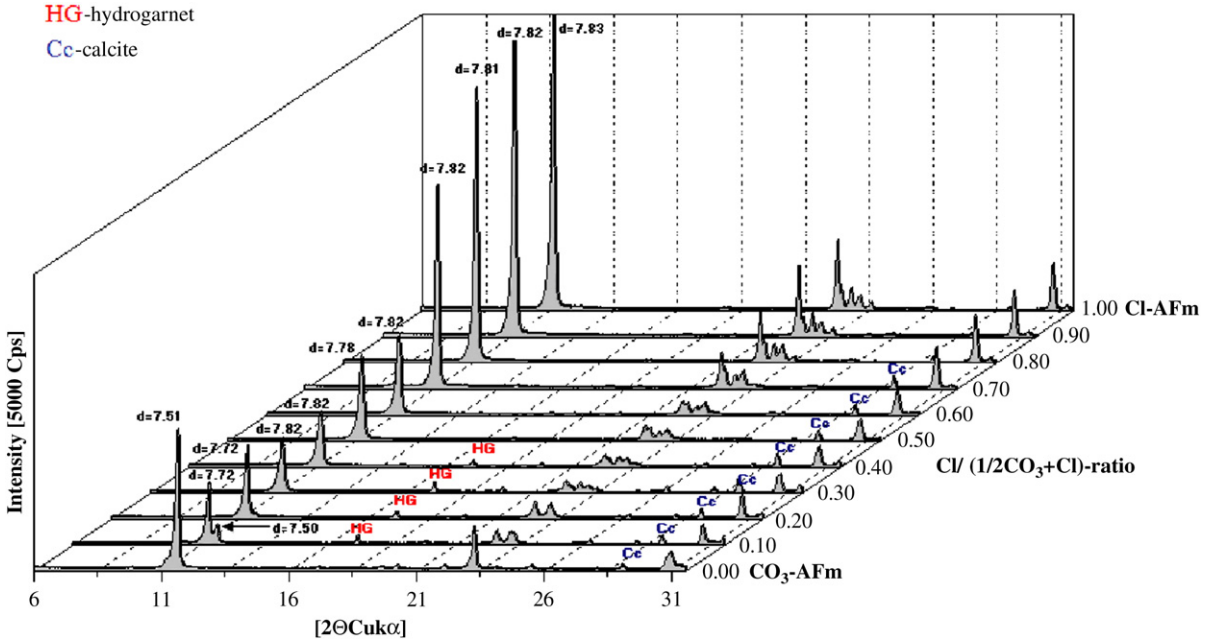

Fig. 5. Partial XRD patterns of the solid solution formation at 25 ± 2 °C between Friedel's salt and monocarboaluminate. Drying at 35% RH does not introduce phase changes. Reflections marked as: HG are attributed to hydrogarnet, Cc are attributed to calcite.

Table 5
Aqueous solution compositions measured from undersaturation for samples between monocarboaluminate (Cl/Al = 0) and Friedel's salt (Cl/Al = 1), and with an excess of $CaCl_2$ (values >1); at 25 ± 2 °C and after 180 days of equilibration.

Calculated Cl/Al- ratio (total system)	Ca [mmol/l] (aq)	Al [mmol/l] (aq)	Cl [mmol/l] (aq)	pH	Solid phase at end of experiment
0.00	3.67	1.59	0.00	11.64	Mc, Cc
0.10	4.14	1.08	0.81	11.56	FS-Mc_{ss}, Mc, Cc
0.20	5.35	1.05	2.02	11.58	FS-Mc_{ss}, Cc
0.30	5.70	0.67	3.47	11.61	FS-Mc_{ss}, Cc
0.40	6.95	0.57	7.60	11.55	FS-Mc_{ss}, Cc
0.50	9.25	0.52	9.87	11.55	FS-Mc_{ss}, Cc
0.60	9.39	0.62	10.72	11.53	FS-Mc_{ss}, Cc
0.70	10.24	1.46	11.97	11.66	FS-Mc_{ss}, Cc
0.80	10.74	1.86	12.42	11.67	FS-Mc_{ss}, Cc
0.90	12.17	1.78	13.13	11.64	FS-Mc_{ss}, Cc
1.05	12.33	1.15	13.37	11.69	n.d.
1.1	13.73	0.91	15.77	11.72	n.d.
1.2	16.88	0.89	24.75	11.64	n.d.

Abbreviations: Mc=monocarboaluminate, Cc=calcite, FS-Mc_{ss}=Friedel's salt in solid solution with monocarboaluminate; n.d.—not determined.

reduced relative to those in the carbonate-free system: Fig. 10(b) compares calculated and measured aqueous compositions. Thus with rising chloride ratio, carbonate is displaced from monocarboaluminate (Fig. 11) forming calcite and Friedel's salt. These calculations are consistent with experimental results reported in the literature [4,78–80].

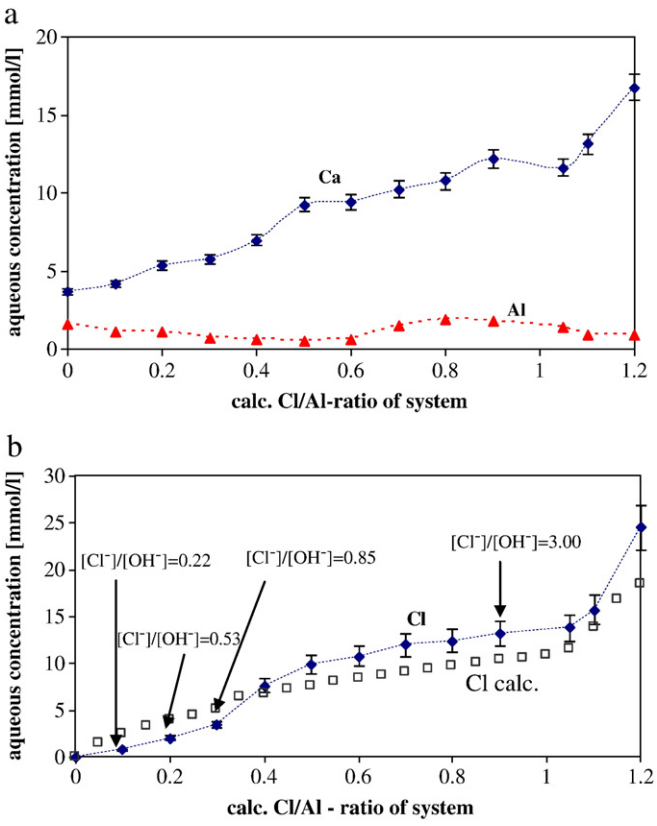

Fig. 6. (a). Equilibrium calcium and aluminium aqueous concentrations, commencing from undersaturation, for solids between monocarboaluminate (Cl/Al = 0) — Friedel's salt (Cl/Al = 1) and with an excess of calcium chloride (values > 1) at 25 ± 2 °C and 180 days of equilibration. Error bars are shown for Ca. (b). Equilibrium chloride aqueous concentrations, commencing from undersaturation for solids between monocarboaluminate (Cl/Al = 0) — Friedel's salt (Cl/Al = 1) and with an excess of calcium chloride (values > 1) at 25 ± 2 °C and after 180 days of equilibration. Error bars are shown for Cl. Variations in the measured aqueous $[Cl^-]/[OH^-]$ ratios are shown at selected points: see Discussion. Open squares represent chloride concentrations calculated by GEMS.

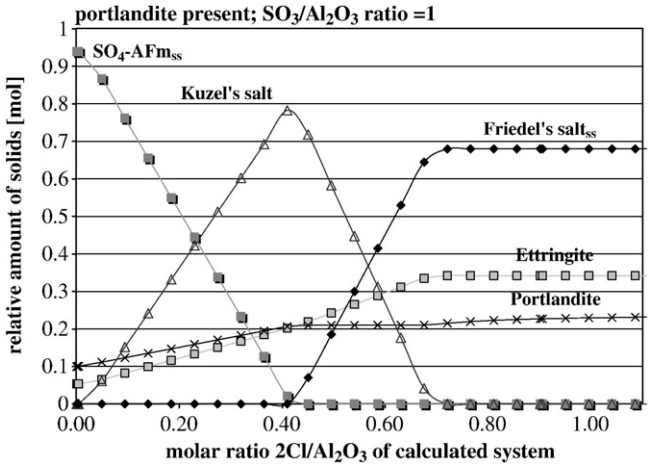

Fig. 7. Relative amount of solid hydrate phases of a hydrated model mixture consisting of initially 1 mol C_3A, excess of portlandite and with fixed initial sulfate ratio ($SO_3/Al_2O_3 = 1$) showing phase development and its dependence on changing chloride ratios ($2Cl/Al_2O_3$) at 25 °C.

4.3. Relationships of Cl, CO_3 and SO_4 AFm phases

Schematic phase relations at 25 °C, between Friedel's salt and other AFm phases are plotted in Fig. 12. To construct this diagram it was assumed that the system contained an excess of both $CaCO_3$ and $Ca(OH)_2$. A limited solid solution between SO_4-AFm/CO_3-AFm and between Kuzel's salt and either/SO_4-AFm or Friedel's salt are admitted. Since the AFm phases also contain minor hydroxide substituted for other anions the diagram is essentially a projection with (OH) substitution (not shown) forming a third dimension. This accords with the mineralogy of many Portland cements during early stages of alteration and has the advantage of fixing approximately the activities of calcium, carbonate and hydroxide. Some details of the phase boundaries are not known precisely but solid solution between SO_4-AFm and CO_3-AFm is known from previous studies to be negligible [2]. Kuzel's salt is incompatible with CO_3-AFm. Taking into the account the above solid solution limits a region of three coexisting phases (SO_4-AFm + Kuzel's salt + Friedel's salt) must exist. However the range of compositions included in this region of coexistence must be physically small. This is because of the existence of the extensive solid solution based on Friedel's salt and CO_3-AFm, shown at the right-hand edge in Fig. 12, and the physical location of points a and b ensures that most of the ternary composition space is occupied by the coexistence of two AFm phases, SO_4-AFm and a carbonate-substituted Friedel's salt. This extensive range of Friedel's salt type solid solution and the resulting broad range of compositions included in this two phase region, explain why Kuzel's salt is only infrequently reported in chloride-containing cement pastes. Kuzel's salt is destabilised by even small amounts of carbonate and will only be encountered in low-carbonate environments.

5. Discussion

5.1. Structure of the phases: carbonate in Friedel's salt

Carbonate, even at low-carbonate activities, has the ability to substitute for chloride in "Friedel's salt". Thus when Friedel's salt is reported it will not necessarily have its theoretical chloride content.

Analysis of changes in the X-ray *d* spacings of solid solution members enables us to predict the orientation of the carbonate group in Friedel's salt by analogy with the structures of other known AFm types. In hemicarboaluminate, the carbonate is oriented normal to the principal $(Ca_2Al(OH)_6)^+$ layers whereas in monocarboaluminate, it is planar [81].

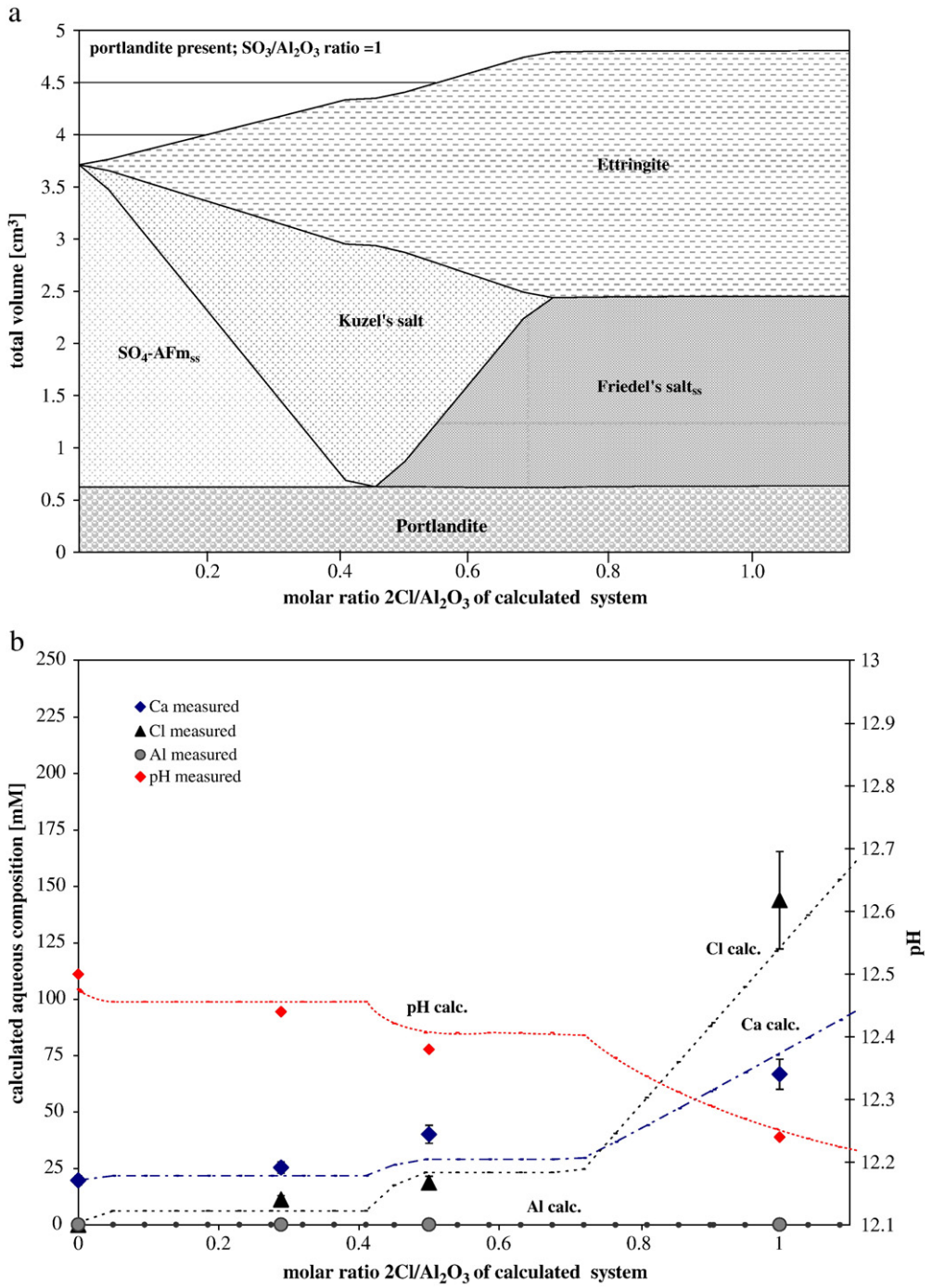

Fig. 8. (a). Calculated total volume of solid phases of a hydrated model mixture initially consisting of 0.01 mol C_3A, 60 ml H_2O, 0.015 mol portlandite and with fixed initial sulfate ratio ($SO_3/Al_2O_3 = 1$) showing phase development and its dependence on changing chloride ratios ($2Cl/Al_2O_3$) at 25 °C. Minor changes in slope at $2Cl/Al_2O_3 \sim 0.4$ probably arise from rounding errors in the calculation. (b). Calculated and experimental aqueous composition of hydrated model mixture initially consisting of 0.01 mol C_3A, 0.015 mol portlandite, 60 ml H_2O and with fixed initial sulfate ratio ($SO_3/Al_2O_3 = 1$) showing its dependence on changing chloride ratios ($2Cl/Al_2O_3$) at 25 ± 2 °C.

Chloride behaves as a simple spherical ion, whereas carbonate is a trigonal planar group and, depending on carbonate orientation, the two possibilities differ in the effective molar volume of the anionic substituent and hence in their contribution to the basal spacing and density e.g., the densities of hemi and monocarboaluminate are affected by the orientation of the trigonal planar carbonate group. Carbonate is most efficiently packed in monocarboaluminate (basal spacing: $d = 7.5$ Å), where it is sub-parallel to the principal layer spacing [82], hence its relatively high density, whereas in hemicarboaluminate (basal spacing: $d = 8.1$ Å), it is perpendicular to the principal layers [62]. In the case of Friedel's salt (spacing: $d = 7.8$ Å) and associated monocarboaluminate solid solutions we do not observe an increase in basal spacing value with increasing carbonate content we can therefore conclude that the carbonate group is essentially parallel or sub-parallel to the principal layer spacing.

5.2. Polymorphism of Friedel's salt

The polymorphism of Friedel's salt is possibly affected by solid solution with OH-AFm. The occurrence of Friedel's salt in M and R phases has been noted [7,13,15,83]. The transformation temperature between M and R is possibly affected by solid solution, with R being

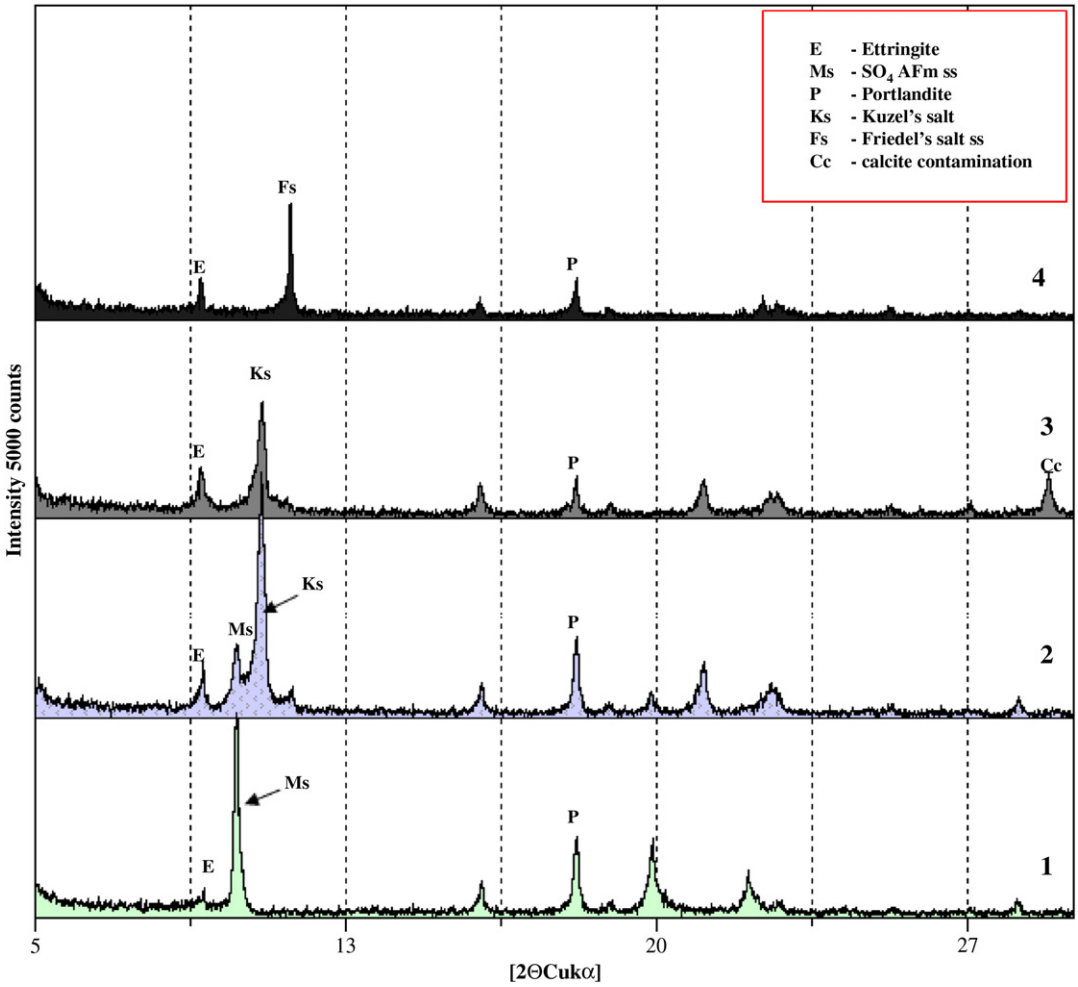

Fig. 9. XRD patterns showing mineralogical changes and influence of $CaCl_2$ addition for the system: 0.01 moles C_3A–0.01 mol $CaSO_4$–0.015 mol $Ca(OH)_2$–60 ml H_2O at 25 ± 2 °C; respectively plots: 1—no $CaCl_2$ present; 2—0.003 mol of $CaCl_2$ added; 3—0.005 mol $CaCl_2$ added; 4—0.01 mol $CaCl_2$ added.

stabilised to progressively lower temperatures by increasing substitution of OH, but the precise dependence of transformation temperature, or range of temperatures, on composition has not been studied. We suppose that R is stabilised to progressively lower temperature by OH substitution and that a wide thermal range of coexistence of the two polymorphs may occur.

5.3. Implication for solid solution formation

Experimental data recorded in the literature [1,6] are often not directly comparable to those of the title study. This is partly because of the different restrains which were used. In experiments performed by Pöllmann [1,6] species activities were controlled by weighted amounts of reactants whereas in the title study, buffer systems [84] like those encountered in commercial cements were used to control activities. For example calcite and hemicarboaluminate are not compatible phases and the hemicarboaluminate will not occur at equilibrium in calcium carbonate-saturated pastes.

Another complication in the interpretation of data arises from the water state of AFm phases. It is known from the lime–alumina–water system that OH-AFm occurs in at least two discrete hydration states, with 13 and $19H_2O$, whereas Friedel's salt, the chloride AFm, seems to be stabilised in only one water state, $10H_2O$. Complete solid solution between Friedel's salt and OH-AFm, after allowing for partial substitution of OH by Cl, could only occur between equivalent water states. Thus where Friedel's salt type solid solution coexists with $19H_2O$ AFm, as occurs in wet samples, differences in water states rules out complete solid solution. We have no definite evidence on the extent of solid solution between lower water states. However interpretations based on the limit of solid solution inferred from dried samples is also suspect, as the lower water state encountered following drying at 35% RH is almost certainly an artefact induced by the drying process.

Friedel's salt formation is a potentially effective way of removing chloride from the pore fluid of a Portland cement. Table 2 shows that in the range of temperatures 5–25 °C, the minimum aqueous chloride concentration necessary to stabilise Friedel's salt is ~6 mM. This means that the ionic strength of the aqueous phase does not much differ from that of a model alkali-free cement and, on that account, the activity of water remains sufficiently high so that the high water variants of OH-AFm are likely to coexist with Friedel's salt type solid solution. Under these conditions, complete solid solution amongst OH and Cl-AFm will not occur.

5.4. Application to commercial Portland cement: binding capacity for chloride

Commercial Portland cement pastes generally start chloride-free: because they contain sulfate and/or carbonate, the initially-formed AFm phase is a SO_4-AFm type, with some sulfate replaced by OH at 25 °C [2] or CO_3-AFm. To estimate the capacity of cement to bind chloride, the contribution from Friedel's salt is limited by two factors: the maximum amount of Friedel's salt which can form and temperature, because Friedel's salt is destabilised with increasing

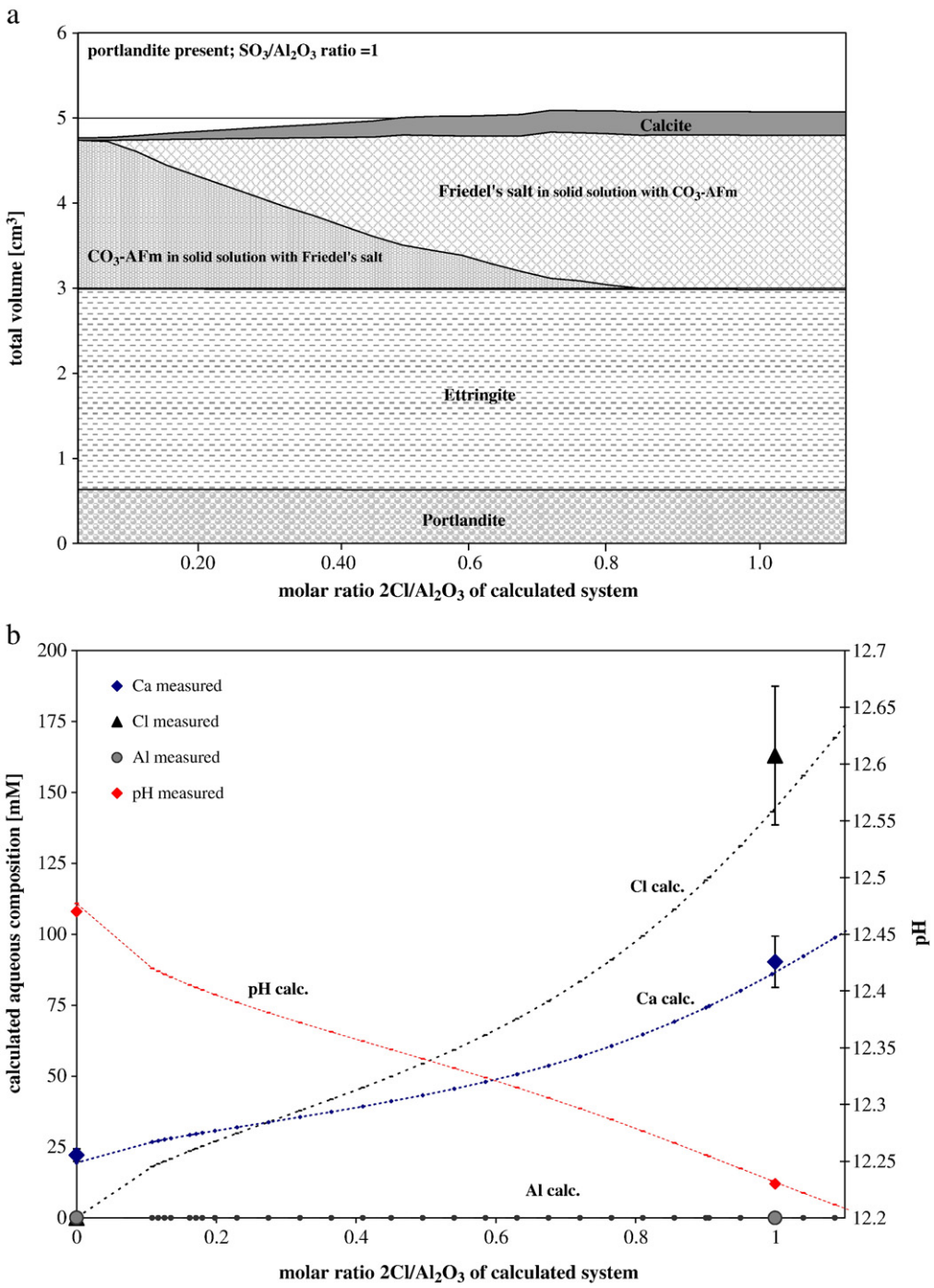

Fig. 10. (a). Total volume of solid phases of a hydrated model mixture initially consisting of 0.01 mol C_3A, 60 ml H_2O, 0.015 mol portlandite, 0.0075 mol $CaCO_3$ and with fixed initial sulfate ratio ($SO_3/Al_2O_3 = 1$) showing phase development and its dependence on changing chloride ratios ($2Cl/Al_2O_3$) at 25 °C. (b). Calculated and experimental aqueous composition of hydrated model mixture initially consisting of 0.01 mol C_3A, 0.015 mol portlandite, 0.0075 mol $CaCO_3$, 60 ml H_2O and with fixed initial sulfate ratio ($SO_3/Al_2O_3 = 1$) showing its dependence on changing chloride ratios ($2Cl/Al_2O_3$) at 25 ± 2 °C.

temperature. At constant temperature, 25 °C, such that Friedel's salt is stable, the binding of chloride is still complex, as chloride must compete with other anions for binding sites in AFm. Moreover the role of C–S–H in binding has to be assessed. To calculate the contribution of AFm to the binding potential, we must place restrictions on the calculations, nevertheless attempting to keep these as generic as possible. The first condition imposed is that the aqueous phase (cement pore fluid) pH is close to 12, as would occur if $Ca(OH)_2$ and/or high calcium C–S–H were present. The second condition is that the activity of sulfate and carbonate are fixed by the equilibration of pore fluid with ettringite and with calcite, respectively. These restrictions are realistic, and enable us to focus on the role of changing chloride concentration.

Where cement is in contact with water high in chloride, and once the AFm phase is saturated with chloride, the amount of Friedel's salt is maximised; no other chloride-binding phase appears until very high chloride concentrations, >3 M, such that oxychlorides become stable [54,65]. Thus Table 2 should not be interpreted as implying that Friedel's salt can only coexist with the Cl molarity shown: it will also coexist to much higher concentrations: what is shown is the minimum critical chloride content necessary to stabilise the solids. However higher chloride concentrations may also destabilise other

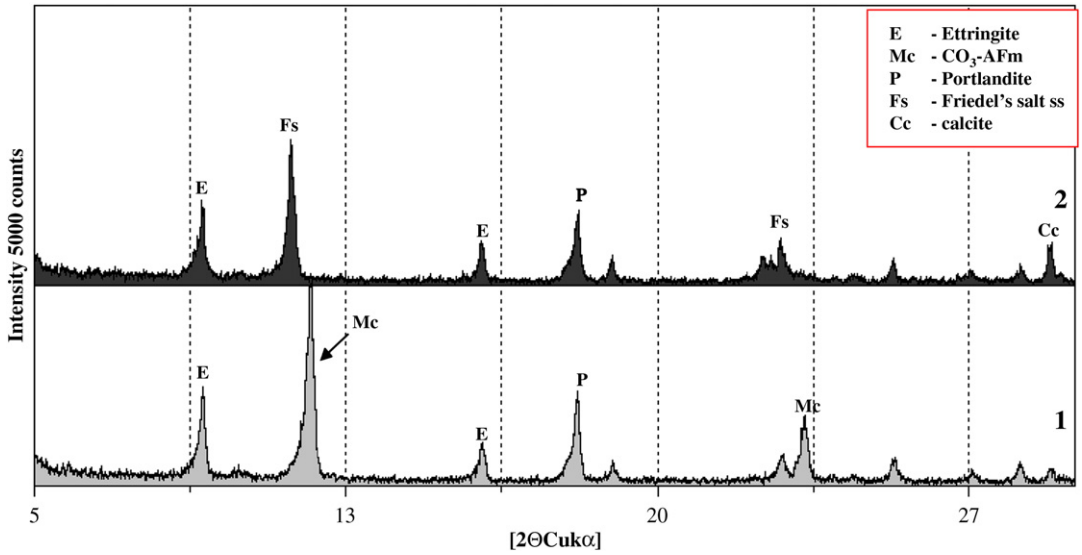

Fig. 11. XRD patterns showing mineralogical changes and influence of $CaCl_2$ addition for the system 0.01 mol C_3A–0.01 mol $CaSO_4$–0.015 mol $Ca(OH)_2$–0.0075 mol $CaCO_3$–60 ml H_2O at 25 ± 2 °C; 1—no $CaCl_2$ present; 2—0.01 mol of $CaCl_2$ added.

phases such as Kuzel's salt or monocarboaluminate and increase bound chloride.

The diagrams presented here are *conditional*, implying that certain restrictions have been placed on their construction and that these conditions have to be respected in order to make valid predictions. It will be appreciated that multi-component systems require more than two dimensions completely to show all features, hence the need for restrictions necessary for accurate two-dimensional graphical representations. However we have attempted to place reasonable sets of restrictions on constructions so as to preserve as many generic features as possible while, at the same time, depicting conditions likely to occur in Portland cements. A future modelling description will include additional factors e.g. chloride sorption on C–S–H and the influence of soluble alkalis on the distribution of chlorides.

The role of Friedel's salt in expansive processes has been discussed in the literature, often without conclusive results. From inspection of trial calculations, Fig. 8(a) shows that the expansion is associated with enhanced ettringite formation as sulfate is displaced from AFm. Under conditions such that ettringite and Friedel's salt both increase in amount, significant increases in molar volume of the solids are predicted to occur. However the presence of reactive carbonate greatly reduces the change in molar volume in the course of Friedel's salt formation and hence the potential for expansion. This is a possible positive argument for including carbonate in cement: to mitigate the expansive potential occurring with chloride ingress. The possibility of developing volume stable cements tailored for service in specific environments needs to be explored in more depth but certainly simplistic association of particular phases as “expansive” or “non-expansive” should be avoided; what is important is the overall volume change associated with the redistribution of chemical substance in response to a mass flux — in this instance, of chloride.

Chloride-induced corrosion of steel is especially likely to occur at aqueous $[Cl^-]/[OH^-]$ ratios above 0.6 such that destruction of the passivating layer occurs [85]. Comparing data in Figs. 3(b) and 6(b),

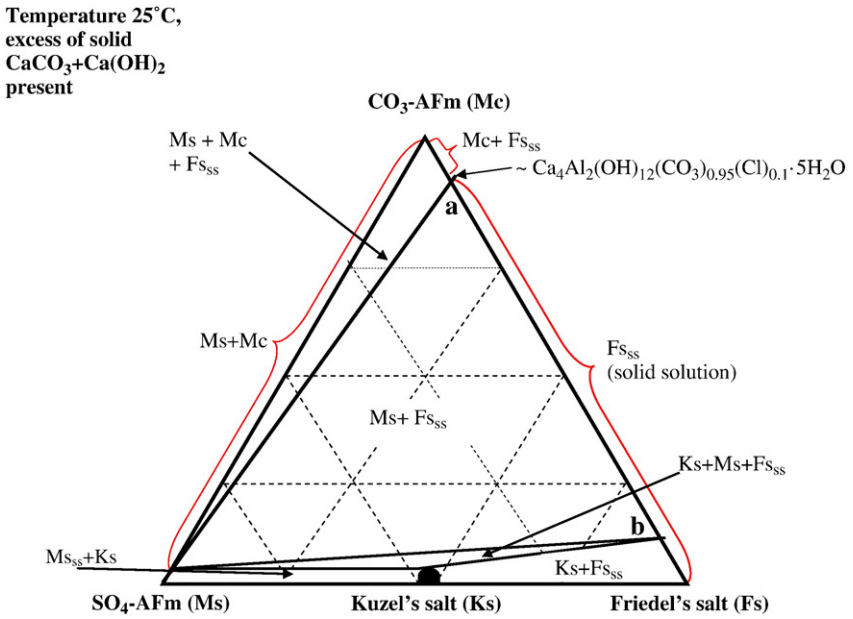

Fig. 12. Schematic phase relations at 25 °C, between Friedel's salt, monosulfoaluminate and monocarboaluminate. Most of the composition range is dominated by the two solid phase region ($Ms + FS_{ss}$).

Table 6
Fraction of chloride bound per g of phase.

Solid phase	wt.% Cl bound per gram of solid phase	Reference
$Ca_4Al_2(OH)_{13.8}(Cl)_{0.2}\cdot 4H_2O$	1.34	This work
$Ca_4Al_2(OH)_{12}(CO_3)_{0.95}(Cl)_{0.1}\cdot 5H_2O$	0.62	This work
$Ca_4Al_2(OH)_{12.05}(Cl)_{1.95}\cdot 4H_2O$	12.33	This work
$Ca_4Al_2(SO_4)_{0.5}(Cl)\ (OH)_{12}\cdot 6H_2O$	5.81	This work
0.68 C/S ratio C–S–H	0.6	[44]
1.91 C/S ratio C–S–H	1.5	[44]

this threshold is achieved with less chloride substitution into the monocarboaluminate than in into hydroxy AFm. This means that for the systems containing calcium carbonate and subject to chloride ingress, depassivation may occur more readily than for the carbonate-free compositions.

Table 6 shows the fraction of chloride per unit mass of cement substance from which it is apparent that the binding potential of C–S–H is not negligible given that it is the most abundant paste constituent but that idealised Friedel's salt is still the most active chloride sorber on a mass basis.

As noted, a comprehensive model is being developed, integrating the contributions of AFm, alkalis and of C–S–H to the overall binding [86].

6. Conclusions

Thermodynamic properties of chloride hydrates: Friedel's salt and Kuzel's salt were determined. Solid solutions have been investigated and compared with data reviewed in the literature. Data indicate solid solution formation between hydroxy AFm and Friedel's salt in the range of $Cl/(Cl+OH)$ ratios: 0.2–1 and solid solution between monocarboaluminate and Friedel's salt for the $Cl/(Cl+1/2CO_3)$ ratios: 0.1–1. No solid solution have been found between Friedel's salt and monosulfoaluminate but instead an ordered compound, Kuzel's salt, $Ca_4Al_2(SO_4)_{0.5}(Cl)(OH)_{12}\cdot 6H_2O$ was encountered.

An equilibrium model of the chloride binding by the AFm and influence on the AFm/AFt mineralogy has been proposed for the systems with and without calcium carbonate. Chloride ions entering the system displace sulfate from monosulfoaluminate forming Kuzel's salt at lower chloride concentrations and Friedel's salt at higher concentrations. Liberated sulfate ions react with calcium and aluminium forming ettringite which can cause volume expansion, or seal pores, or both. Chloride ions also have the ability to displace carbonate from the monocarboaluminate phase and forming Friedel's salt but this reaction does not cause as much change in the molar volume: the carbonate ions form calcite. If we compare plain and carbonate-containing systems, a trade-off occurs. Carbonate suppresses potentially expansive reactions from chloride ingress but at the same time reduces the total capacity to bind chloride and increases aqueous $[Cl^-]/[OH^-]$ ratios.

The notation used on graphs

SO_4-AFm monosulfoaluminate
Cl-AFm Friedel's salt
CO_3-AFm monocarboaluminate
OH-AFm hydroxy AFm.

Acknowledgments

Magdalena Balonis is grateful to the European Community under the Marie Curie Research Training Network MRTN-CT-2005-019283 “Fundamental understanding of cementitious materials for improved chemical physical and aesthetic performance” (http://www.nanocem.org/MC-RTN/) for the full support of MC project 1. The authors would like to thank to: Dr. Dimitri Kulik (PSI, Switzerland) for his help with GEMS software and Prof. Mette Geiker (DTU, Denmark) for stimulating discussions regarding chloride binding in cementitious systems.

References

[1] H. Pöllmann, Incorporation of SO_4^{2-}, and CO_3^{2-} and OH^- in hydration products of tricalciumaluminate, International Congress on the Chemistry of Cement, New Dehli, 1992, pp. 361–369, Vol. 4.
[2] T. Matschei, B. Lothenbach, F.P. Glasser, The AFm phase in Portland cement, Cement and Concrete Research 37 (2) (2007) 118–130.
[3] H. Pöllmann, Solid solution of complex aluminate hydrates containing Cl^-, OH^- and CO_3^{2-} anions, 8th International Congress on the Chemistry of Cement, Rio de Janeiro, 1986, pp. 300–306, Vol. 3.
[4] E. Nielsen, D. Herfort, M. Geiker, D. Hooton, Effect of solid solution of AFm phases on chloride binding, Proceedings, 11th Int. Congress on the Chemistry of Cement, South Africa, 2003.
[5] F.P. Glasser, A. Kindness, S.A. Stronach, Stability and solubility relationships in AFm phases Part I. Chloride, sulfate and hydroxide, Cement and Concrete Research 29 (1999) 861–866.
[6] H. Pöllmann, Solid soution of complex calcium aluminate hydrates containing Cl^-, OH^- and CO_3^{2-} - anions, Proc. 8th Int. Symp. on the Chem. of Cement, Rio de Janeiro, 1986, pp. 300–306, Vol. 3.
[7] H.J. Kuzel, Röntgenuntersuchung in System $3CaO\cdot Al_2O_3\cdot CaSO_4\cdot nH_2O$–$3CaO\cdot Al_2O_3\cdot CaCl_2\cdot nH_2O$–$H_2O$, Neues Jahrbuch für Mineralogie Monatshefte, 1966, pp. 193–200.
[8] R.V. Gaines, H.C.W. Skinner, E.E. Foord, B. Mason, A. Rosenzweig, Dana's New Mineralogy, Eighth edition, John Wiley & Sons, New York, 1997, pp. 1573–1586.
[9] M. Sacerdoti, E. Passaglia, Hydrocalumite from Latium, Italy: its crystal structure and relationship, with related synthetic phases, Locality: Montalto di Castro, Viterbo, Latium, Italy Neues Jahrbuch fur Mineralogie Monatshefte, 1988, pp. 462–475.
[10] H. Pöllmann, T. Witzke, H. Kohler, Kuzelite, American Mineralogist (1998) 909 abstract.
[11] H. Pöllmann, Characterization of different water contents of ettringite and kuzelite, Proc. XII International Congress on the Chemistry of Cement, Montreal, Canada, 2007, CD.
[12] U.A. Birnin-Yauri, F.P. Glasser, Friedel's salt, $Ca_2Al(OH)6(Cl, OH)\cdot 2H_2O$: its solid solutions and their role in chloride binding, Cement and Concrete Research 28 (12) (1998) 1713–1723.
[13] J.P. Rapin, E. Elkaim, M. Francois, G. Renaudin, Structural transition of Friedel's salt $3CaO\cdot Al_2O_3\cdot CaCl_2\cdot 10H_2O$ studied by synchrotron powder diffraction, Cement and Concrete Research 32 (2002) 513–519.
[14] Matschei, T., Lothenbach B., Glasser F.P., The role of calcium carbonate in cement hydration 2007; 37(4): 551–558.
[15] S. Chatterjee, Mechanism of the $CaCl_2$ attack on Portland cement concrete, Cement and Concrete Research 8 (1978) 461–468.
[16] M. Conjeaud, Mecanisme d'attaque des Ciments Portland par $CaCl_2$, Semin. Intern, Torino, Italy, 1982.
[17] V.S. Ramachandran, Concrete Admixtures Handbook: Properties, Science and Technology, Noyes Publications, 1984.
[18] B.E.I. Abdelrazig, D.G. Bonner, D.V. Nowell, J.M. Dransfield, P.J. Egan, The solution chemistry and early hydration of ordinary Portland cement pastes with and without admixtures, Thermochimica Acta 340–341 (1999) 41–430.
[19] C. Andrade, Calculation of chloride diffusion coefficients in concrete from ionic migration measurements, Cement and Concrete Research 23 (3) (1993) 724–742.
[20] P. Brown, J. Bothe Jr., The system CaO–Al_2O_3–$CaCl_2$–H_2O at 23 ± 2 °C and the mechanisms of chloride binding in concrete, Cement and Concrete Research 34 (2004) 1549–1553.
[21] J. Csizmadia, G. Balazs, F.D. Tamas, Chloride ion binding capacity of aluminoferrites, Cement and Concrete Research 31 (4) (2001) 577–588.
[22] A. Delagrave, J. Marchand, J.P. Ollivier, S. Julien, K. Hazrati, Chloride binding capacity of various hydrated cement paste systems, Advanced Cement Based Materials 6 (1) (1997) 28–35.
[23] R.K. Dhir, M.A.K. El-Mohr, T.D. Dyer, Chloride binding in GGBS concrete, Cement and Concrete Research 26 (12) (1996) 1767–1773.
[24] M. Geiker, E.P. Nielsen, D. Herfort, Prediction of chloride ingress and binding in cement paste, Materials and Structures 40 (2007) 405–417.
[25] H. Hirao, K. Yamada, H. Takahashi, H. Zibara, Chloride binding of cement estimated by binding isotherms of hydrates, Journal of Advanced Concrete Technology 3 (1) (2005) 77–84.
[26] K. Kopecskó, Gy. Balázs, Chloride ion binding of steam cured aluminates and cements, Symposium Dubrovnik, Croatia, 20–23 May 2007. Concrete Structures — Stimulators of Development, Dubrovnik, 2007.
[27] W. Kurdowski, L. Taczuk, B. Trybalska, Behaviour of high alumina cement in chloride solutions, in: R.J. Mangabhai (Ed.), Calcium Aluminate Cements, E & FN Spon, London, 1990, pp. 222–229.
[28] T. Luping, L.O. Nilsson, Chloride binding capacity and binding isotherms of OPC pastes and mortars, Cement and Concrete Research 23 (2) (1993) 247–253.
[29] E.P. Nielsen, D. Herfort, M.R. Geiker, Binding of chloride and alkalis in Portland cement systems, Cement and Concrete Research 35 (2005) 117–123.
[30] H.E. Schwiete, U. Ludwig, Combining of calcium chloride and calcium sulphate in hydration of aluminate–ferrite clinker constituents, Zement Kalk Gips 22 (1969) 225–234.
[31] T. Sumranwanich, S. Tangtermsirikul, A model for predicting time-dependent chloride binding capacity of cement–fly ash cementitious system, Materias and Structures 37 (2004) 387–396.

[32] A.K. Suryavanshi, J.D. Scantlebury, S.B. Lyon, The binding of chloride ions by sulphate resistant Portland cement, Cement and Concrete Research 25 (3) (1995) 581–592.
[33] J. Tritthart, Chloride binding in cement, II the influence of the hydroxide concentration in the pore solution of hardened cement paste on chloride binding, Cement and Concrete Research 19 (1989) 683–691.
[34] Y. Xu, The influence of sulphates on chloride binding and pore solution chemistry, Cement and Concrete Research 27 (12) (1997) 1841–1850.
[35] Q. Yuan, C. Shi, G. De Schutter, K. Audenaert, D. Deng, Chloride binding of cement-based materials subjected to external chloride environment — a review, Construction and Building Materials 23 (2009) 1–13.
[36] Zibara, H., Binding of external chlorides by cement pastes. PhD-Thesis, University of Toronto, Canada, 2001.
[37] H. Zibara, D. Hooton, K. Yamada, M.D.A. Thomas, Roles of cement mineral phases in chloride binding, Cement Science and Concrete Technology 56 (2002) 384–391.
[38] P. Gégout, E. Revertégat, G. Moine, Action of chloride ions on hydrated cement pastes: influence of the cement type and long time effect of the concentration of chlorides, Cement and Concrete Research 22 (1992) 451–457.
[39] W. Richartz, Die Bindung von Chlorid bei Zementerhärtung, Zement Kalk Gips 10 (1969) 447–456.
[40] R. Fischer, H.J. Kuzel, H. Schellhorn, Hydrocalumit, Mischkristalle von 'Friedelschem Salz' $3CaO\cdot Al_2O_3\cdot CaCl_2\cdot 10H_2O$' und Tetrecalciuminathydrat? Neues Jahrbuch für Mineralogie Monatshefte 7 (1982) 322–334.
[41] Pöllmann, H., Mischkristallbildung in den Systemen $3CaO\cdot Al_2O_3\cdot CaCl_2\cdot 10H_2O$–$3CaO\cdot Al_2O_3\cdot CaCO_3\cdot 11H_2O$ und $3CaO\cdot Al_2O_3\cdot CaCl_2\cdot 10H_2O$–$3CaO\cdot Al_2O_3\cdot Ca(OH)_2\cdot 12H_2O$ Diploma Thesis, 1980.
[42] Hobbs, M., Solubilities and ion exchange properties of solid solutions between the OH, Cl and CO_3 end members of the monocalcium aluminate hydrates. PhD-Thesis, University of Waterloo, Canada, 2001.
[43] Vialis Terrisse, H., Interaction des Silicates de Calcium Hydratés, principaux constituants du ciment, avec les chlorures d'alcalins. Analogie avec les argiles. Ph.D Thesis (in french), Université de Bourgogne, France, 2000.
[44] J.J. Beaudoin, V.S. Ramachandran, R.F. Feldman, Interaction of chloride and C–S–H, Cement and Concrete Research 20 (1990) 875–883.
[45] C.L. Page, N.R. Short, A. El Tarras, Diffusion of chloride ions in hardened cement pastes, Cement and Concrete Research 11 (3) (1981) 395–406.
[46] C.L. Page, N.R. Short, W.R. Holden, Materials Research Group, The influence of different cements on chloride-induced corrosion of reinforcing steel, Cement and Concrete Research 16 (1986) 79–86.
[47] S. Diamond, Chloride concentrations in concrete pore solutions resulting from calcium and sodium chloride admixtures, Cement, Concrete and Aggregates 8 (2) (1986) 97–102.
[48] O.A. Kayyali, M.N. Haque, Chloride penetration and the ratio of Cl^-/OH^- in the pores of cement paste, Cement and Concrete Research 18 (1988) 895–900.
[49] B. Lothenbach, E. Wieland, A thermodynamic approach to the hydration of sulphate-resisting Portland cement, Waste Management 26 (2006) 706–719.
[50] B. Lothenbach, F. Winnefeld, Thermodynamic modelling of the hydration of Portland cement, Cement and Concrete Research 36 (2006) 209–226.
[51] B. Lothenbach, T. Matschei, G. Möschner, F.P. Glasser, Thermodynamic modelling of the effect of temperature on the hydration and porosity of Portland cement, Cement and Concrete Research 38 (2008) 1–18.
[52] Matschei, T., Thermodynamics of Cement Hydration. Ph.D thesis, University of Aberdeen, UK, 2007.
[53] T. Matschei, B. Lothenbach, F.P. Glasser, Thermodynamic properties of Portland cement hydrates in the system $CaO–Al_2O_3–SiO_2–CaSO_4–CaCO_3–H_2O$, Cement and Concrete Research 37 (2007) 1379–1410.
[54] D. Damidot, U.A. Birnin-Yauri, F.P. Glasser, Thermodynamic investigation of the $CaO–Al_2O_3–CaCl_2–H_2O$ system at 25 °C and the influence of Na_2O, IL Cemento 91 (1994) 243–254.
[55] H. Pöllmann, H.J. Kuzel, R. Wenda, Compounds with ettringite structure, Neues Jahrbuch für Mineralogie Abhandlungen 160 (1989) 133–158.
[56] H.E. Schwiete, U. Ludwig, J. Albreck, Bindung von Calciumchlorid bei Hydratation der aluminatisch-ferritischen Bestandteile des Portlandzementes, Die Naturwissenschaften 55 (4) (1968) 179.
[57] H.E. Schwiete, U. Ludwig, Crystal structures and properties of cement hydration products (hydrated calcium aliuminates and ferrites), Fifth Int. Symp. On the Chem. Of Cement, Tokyo, Japan, 1968, pp. 37–67.
[58] M. Ben Yair, Studies on the stability of calcium chloroaluminate, Israel Journal of Chemistry 9 (1971) 529–536.
[59] J. Bensted, Chloroaluminates and the role of calcium chloride in accelerated hardening of Portland cement, World Cement Technology (1977 Sept.–Oct) 171–175.
[60] F.M. Lea, The Chemistry of Cement and Concrete, Third editionEdward Arnold (Publishers) Ltd, 1970.
[61] D. Kulik, U. Berner, E. Curti, Modelling chemical equilibrium partitioning with the GEMS-PSI code, PSI Scientific Report 4 (2003) 109–122 http://gems.web.psi.ch.
[62] M. Balonis, F.P. Glasser, The density of cement phases, Cement and Concrete Research 39 (2009) 733–739.
[63] H.C. Helgeson, J.M. Delany, H.W. Nesbitt, D.K. Bird, Summary and critique of the thermodynamic properties of rock forming minerals, American Journal of Science 278-A (1978) 229.
[64] M.D. Andersen, H.J. Jakobsen, J. Skibsted, Characterization of the α–β phase transition in Friedels salt ($Ca_2Al(OH)_6Cl\cdot 2H_2O$) by variable-temperature 27Al MAS NMR spectroscopy, The Journal of Physical Chemistry A 106 (28) (2002) 6676–6682.
[65] Birnin-Yauri, U.A., Chloride in cement: study of the system $CaO–Al_2O_3–CaCl_2–H_2O$. Ph.D Thesis, University of Aberdeen, UK, 1993.
[66] J.V. Bothe Jr, P.W. Brown, PhreeqC modeling of Friedel's salt equilibria at 23 ± 1 °C, Cement and Concrete Research 34 (2004) 1057–1063.
[67] D.A. Kulik, M. Kersten, Aqueous solubility diagrams for cementitious waste stabilization systems: II, end-member stoichiometries of ideal calcium silicates hydrate solid solutions, Journal of the American Ceramic Society 84 (12) (2001) 3017–3026.
[68] D.E. Macphee, S.J. Barnett, Solution properties of solids in the ettringite–thaumasite solid solution series, Cement and Concrete Research 34 (2004) 1591–1598.
[69] G. Möschner, B. Lothenbach, F. Winnefeld, A. Ulrich, R. Figi, R. Kretzschmar, Solubility of Fe-ettringite and its solid solutions with Al-ettringite, Proceedings of the 12th Intern. Congress on the Chemistry of Cements, Montreal, 2007.
[70] G. Möschner, B. Lothenbach, F. Winnefeld, A. Ulrich, R. Figi, R. Kretzschmar, Solid solution between Al-ettringite and Fe-ettringite ($Ca_6[Al_{1-x}Fe_x(OH)_6]_2(SO_4)_3\cdot 26H_2O$), Cement and Concrete Research 39 (6) (2009) 482–489.
[71] Bruno, J., et al., Chemical Thermodynamics Vol. 10. Chemical Thermodynamics of Solid Solutions of Interest in Nuclear Waste Management, ed. O.N.E.A.D. Bank. 2007, Amsterdam, The Netherlands: North Holland Elsevier Science Publishers B.V.
[72] E. Curti, Coprecipitation of radionuclides with calcite: estimation of partition coefficients based on a review of laboratory investigations and geochemical data, Applied Geochemistry 14 (4) (1999) 433–445.
[73] H. Pöllmann, H.J. Kuzel, Synthesis and polymorphic transformations of solid solutions in the system $3CaO\cdot Al_2O_3\cdot CaCl_2\cdot nH_2O$–$3CaO\cdot Al_2O_3\cdot Ca(OH)_2\cdot nH_2O$–$H_2O$, Neues Jahrbuch für Mineralogie Monatshefte, 1988, pp. 193–202.
[74] M.H. Roberts, Calcium aluminate hydrates and related basic salt solid solutions, Proc. Fifth Int. Symp. On the Chem. Of Cement, Tokyo, Japan, Supplementary Paper II, 1968, pp. 104–117.
[75] R. Turriziani, G. Schippa, Contribution to the knowledge of hydrated calcium chloro-aluminates, Ricerca Scientifica 25 (1955) 3102–3106.
[76] Stronach, S.A., Thermodynamic Modelling and Phase Relations of Cementitious Systems. Ph.D Thesis, University of Aberdeen, UK, 1996.
[77] H. Hirao, Current state of the studies on chloride binding by cement (draft), Committee of literature survey, Material Div, 2003.
[78] Allan, I., Herfort, D., The mineralogy of chloride attack on concrete with limestone filler. unpublished paper, Aalborg Portland, 2009.
[79] Nielsen, E.P., The durability of white Portland cement to chemical attack. Ph.D Thesis, DTU, Denmark, 2004.
[80] R. Loser, B. Lothenbach, A. Leemann, M. Tuchschmid, Chloride resistance of concrete and its binding capacity — comparison between experimental results and thermodynamic modeling, Cement & Concrete Composites 32 (1) (2010) 34–42.
[81] H.F.W. Taylor, Cement Chemistry (2nd edition), Thomas Telford Publishing, London, 1997.
[82] Renaudin, G., Ph.D thesis (in French), University of Henri Poincaré, Nancy, France, 1998: p. 150.
[83] G. Renaudin, F. Kubel, J.P. Rivera, M. Francois, Structural phase transition and high temperature phase structure of Friedel's salt, $3CaO\cdot Al_2O_3\cdot CaCl_2\cdot 10H_2O$, Cement and Concrete Research 29 (1999) 1937–1942.
[84] T. Matschei, F.P. Glasser, Temperature dependence, 0 to 40 °C, of the mineralogy of Portland cement paste in the presence of calcium carbonate, Cement and Concrete Research 40 (5) (2010) 763–777.
[85] C. Alonso, C. Andrade, M. Castellote, P. Castro, Chloride threshold values to depassivate reinforcing bars embedded in a standardized OPC mortar, Cement and Concrete Research 30 (7) (2000) 1047–1055.
[86] Lothenbach, B., Balonis, M., Geiker, M., Glasser, F.P., Thomas, M.D.A., ooton, D., Chloride binding in cements. Under development for submission, 2010.